ELSEVIER

Chemical Physics 204 (1996) 353–363

Chemical Physics

Molecular force fields of uracil and thymine, through neutron inelastic scattering experiments and scaled quantum mechanical calculations [1]

A. Aamouche [a], G. Berthier [b,*], C. Coulombeau [c], J.P. Flament [d], M. Ghomi [a], C. Henriet [e], H. Jobic [f], P.Y. Turpin [a]

[a] *Laboratoire de Physicochimie Biomoléculaire et Cellulaire, CNRS URA 2056, Institut Curie, 11, rue Pierre et Marie Curie, F-75231 Paris Cedex 05, France*

[b] *Institut de Biologie Physicochimique, 13 rue Pierre et Marie Curie, F-75231 Paris Cedex 05, France*

[c] *Laboratoire d'Etudes Dynamique et Structurale de la Sélectivité, CNRS URA 332, Université J. Fourier, BP 53X, F-38041 Grenoble, France*

[d] *Laboratoire de Dynamique Moléculaire et Photonique, CNRS URA 779, Université de Lille 1, F-59655 Villeneuve d'Ascq, France*

[e] *Cray-Research France, 18 rue de Tilsitt, F-75017 Paris, France*

[f] *Institut de Recherche sur la Catalyse, 2 avenue A. Einstein, F-69626 Villeurbanne, France*

Received 28 January 1995

Abstract

Neutron inelastic scattering (NIS) data have been obtained from polycrystalline samples of pyrimidine nucleic bases, i.e. uracil (U) and thymine (T). These spectra and those previously recorded by optical techniques (Raman scattering and infrared absorption) led us to carry out ab initio quantum mechanical calculations (SCF + MP2) in using split-valence gaussian sets with different d-orbital polarization functions for carbon, nitrogen and oxygen. The F_x matrices (interatomic force constant matrices on the basis of cartesian coordinates) derived from these ab initio calculations have been then described in terms of internal molecular coordinates, allowing vibrational normal modes to be assigned in the framework of the so-called Wilson GF-matrix method. In addition, atomic displacements estimated from the normal mode calculations have been used to simulate the first-order NIS intensities by only considering the fundamentals of the internal molecular vibrational motions. For both molecules (U and T), the internal vibrational modes are located at higher wavenumbers than the lattice vibrational modes (external vibrational motions). In order to scale the calculated vibrational modes the so-called Pulay method has been used. A good agreement between calculated and experimental data (vibrational wavenumbers as well as NIS intensities) has been obtained for most of the internal vibrational modes.

1. Introduction

Neutron inelastic scattering (NIS) is now considered as a powerful tool in order to analyse the vibrational modes of nucleic acid fragments (bases, nucleosides and nucleotides) in solid state phase. NIS presents several advantages over optical spectroscopic methods (Raman scattering and infrared absorption) for investigating molecular vibrations. First, no selection rule has to be applied to the interaction between the incident neutron and molecular vibra-

* Corresponding author.

[1] Dedicated to Professor B. Pullman.

SSDI 0301-0104(95)00298-7

tions. Second, since the inelastic cross-section of hydrogen atoms is much higher than that of other atoms, vibrational modes in which hydrogen motions participate give NIS bands having much higher intensities than those in which they do not. Consequently, in NIS spectra the modes mainly involving heavy atom motions are either not observed or are very weak by comparison with those involving hydrogen vibrations. In addition, NIS spectroscopy is quite appropriate to analyse low wavenumber vibrational modes; this is reflected in the Debye–Waller factor involved in the formulation of NIS cross-sections [1], which also expresses that the mode intensities are enhanced when the temperature is lowered. However, NIS intensities considerably decrease in the wavenumber region higher than 1000 cm^{-1}, owing to a reduced statistics arising from a decrease of the scattered neutron flux, as well as to an additional instrument effect in this spectral region. In the case of nucleic acid bases, the most intense NIS modes below 1000 cm^{-1} are assigned to out-of-plane vibrational modes [1,2] which cannot be as completely analysed by optical spectroscopies. Nevertheless, the major disadvantage of NIS lies in the low intensity of the inelastically scattered beam; thus, a considerable amount of sample is necessary (1–3 g) to run NIS spectra.

In a series of recent investigations, we have reported NIS spectra of nucleic acid purine bases: adenine [1] and guanine [2], and also tetrahydrofuran [3–5] considered as a simple molecular model for sugar vibrational mode analysis, along with normal mode assignments of these molecules. Here, we report NIS spectra obtained at low temperature ($T =$

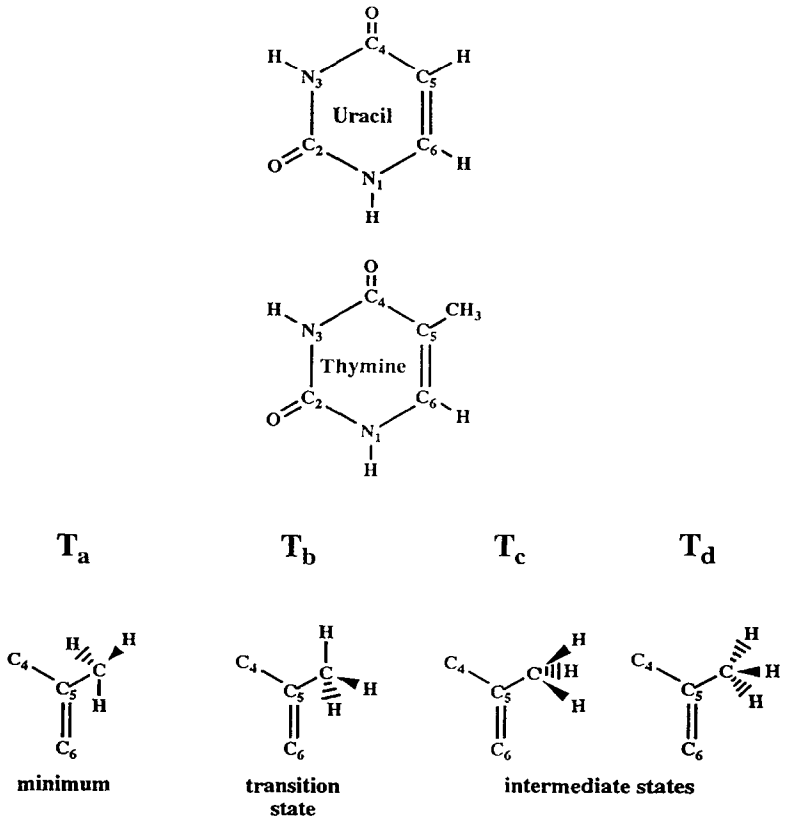

Fig. 1. Chemical structure and atom numbering for uracil and thymine. Various privileged conformations of the methyl group of thymine, noted as T_a, T_b, T_c and T_d, are also drawn (lower part, see also text).

15 K) from polycrystalline samples of uracil and thymine, i.e. pyrimidine bases found in RNA and DNA, respectively.

On the other hand, numerous experimental investigations have been devoted to the vibrational analysis of nucleic acid bases in various phases, by using optical spectroscopies. As far as uracil and thymine are concerned, Raman and infrared spectra from polycrystalline samples [6–10], from argon and nitrogen matrix [11–16] and from aqueous phase [8] are worthwhile to be reminded.

Since 1960 a large amount of theoretical data has been issued in the literature on the electronic structure and properties of nucleic acids bases (specially U and T). It includes semi-empirical studies by Hückel, Parr–Pariser–Pople or other ZDO methods [17–22] as well as by ab initio studies at the simplest level [23]. The vibrational properties of these molecules have been investigated much later [16,24,25]. It is now established that extended basis sets of atomic orbitals as well as correlation effects have to be considered, in order to obtain reliable results as concerns both molecular geometries and vibrational normal mode wavenumbers. To our knowledge, all the theoretical studies published until now on the vibrational spectra of uracil and thymine have been performed at the SCF level in connection with IR and Raman experimental data. For instance, one can mention those calculations performed with minimal atomic bases [10,14,24,25], with split valence sets [14–16] or recently with more extended bases [13]. In all these works, the main aim was to interpret vibrational spectra in assigning only experimental wavenumbers.

In the present work, the spectral features are assigned by using a scaled quantum mechanical (SQM) force field at SCF + MP2 level, which enables both NIS vibrational wavenumbers and spectral intensities to be simulated.

2. Experimental and theoretical methods and results

2.1. Experimental section

Uracil (U) and thymine (T) bases (Fig. 1) were purchased from SIGMA and used as supplied. NIS spectra of these molecules have been obtained on the time-focused crystal analyser spectrometer TFXA

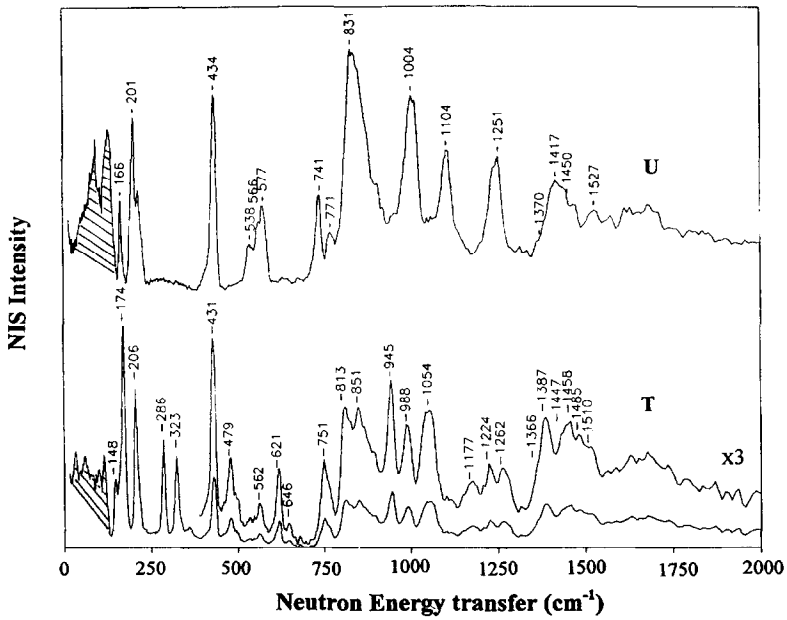

Fig. 2. NIS spectra of uracil (U) and thymine (T) in the spectral region below 2000 cm^{-1}, recorded at $T = 15$ K from polycrystalline samples. Hatched part: lattice spectrum (corresponding to external modes). In order to compare easily U and T NIS bands, the thymine spectrum has been redrawn when multiplied by a factor of three, in the spectral region above 400 cm^{-1}.

located at the ISIS pulsed neutron source of the Rutherford Appleton Laboratory (RAL), UK [26,27]. To record these spectra, approximately 3g of polycrystalline powder of each compound were conditioned in a thin-wall aluminium container. The temperature of experiment was set sufficiently low ($T =$ 15 K) in order to sharpen the vibrational fundamental lines: this is reflected in the Debye–Waller factor of the NIS formulation [28].

Traces U and T of Fig. 2 show the NIS spectra of uracil and thymine, respectively, in the spectral region below 2000 cm^{-1}. The narrow shape of the bands led us to assume that internal (molecular) and external modes (lattice or crystal phonon modes) occur in two distinct spectral regions: all of the bands located below ≈ 120 cm^{-1} can be assigned to external modes which generally give rise to intense and incompletely resolved bands (hatched in Fig. 2). It should be noted that in the case of the purine bases [1,2], external and internal modes are also located in two distinct spectral regions. We may consequently conclude that it is a common feature for all nucleic acid bases, which considerably simplifies the internal and external modes processing (and also their mutual interactions).

Experimental vibrational wavenumbers of U and T (from both NIS and optical spectroscopies) have been reported in Tables 2 and 3, respectively.

2.2. Theoretical section

The quantum chemical calculations have been carried out in using the GAUSSIAN92 code optimized on a Cray C90 supercomputer platform. Post-processing of the vibrational modes has been made on the basis of the Wilson GF-method [29] by using a home-made program (BORNS) allowing F_X (cartesian force constants) to F_R (force constants as defined on the molecular internal coordinates) matrix conversion, redundancy treatment [30], scaling of force-constants by the so-called Pulay method [31,32], simulation of NIS spectral intensities and visualisation of vibrational modes, to be performed.

2.2.1. Basis functions and geometry optimization

Electronic wavefunctions from which force constants and normal mode wavenumbers have been computed, were obtained after complete optimization of the geometry parameters at SCF + MP2 level, by using polarized split valence basis sets, i.e. 6-31G or D95V sets of the GAUSSIAN program [33,34] implemented by d functions with 0.75, 0.80 and 0.85 exponents for carbon, nitrogen and oxygen atoms, respectively. The same procedure has been followed in our previous studies on tetrahydrofuran [3,4]. The calculated geometrical parameters are in very good agreement with those obtained experimentally [35,36].

It has been verified that the calculated results (vibrational wavenumbers and NIS intensities) were not significantly sensitive to the addition of p-polarization functions on the hydrogen atoms. For the sake of briefness, here we only present the results obtained with polarized 6-31G basis set. Quite similar results have been obtained with D95V functions.

Disregarding the hydrogen atoms of the CH_3 substituent of thymine, U and T have planar geometries. The local arrangement of the proper CH_3 group of thymine with respect to the conjugated pyrimidine ring can be described by four privileged conformations: two of them are of C_s symmetry, with one hydrogen in the ring plane (oriented towards C6 or C4 atoms, respectively), the other two hydrogens being symmetrically placed with respect to the heterocyclic ring plane (conformations noted as T_a and T_b in Fig. 1). The other two privileged conformations involve three non-planar hydrogens, one below and the other two above (or vice versa) the molecular ring plane (conformations noted as T_c and T_d in Fig. 1).

In fact, the lower C_s conformation T_a corresponds to the minimum of the potential energy curve with a phase period of 120 degrees, as generated by the motion of the methyl group hindered rotation, while T_b corresponds to a so-called transition state. Finally both T_c and T_d represent intermediate conformations (Table 1).

2.2.2. SQM internal force field

In order to obtain a better agreement between experimental and calculated results we have improved, through the Pulay method [31,32], the quantum mechanical force fields of U and T molecules provided by GAUSSIAN. In a first step the GAUSSIAN F_x matrix has been expressed in terms of internal coordinates (bond stretchings, angular bend-

ings, out-of-plane waggings and torsions), so as to obtain the F_R matrix. Then each diagonal element of F_R has been corrected by a multiplying factor C_{ii} (i denotes one of the internal coordinates of the molecule), commonly called 'force constant scaling factor'. Any off-diagonal term of the F_R matrix, reflecting the interaction between internal i and j coordinates, is corrected by the geometrical mean of C_{ii} and C_{jj} factors (i.e. $C_{ij} = (C_{ii}C_{jj})^{1/2}$). In the course of the force field correction by a least-squares method, attention has been payed to improve both vibrational wavenumbers and NIS intensities.

2.2.3. Calculated wavenumbers and assignments

The vibrational modes of U and T have been calculated by using the C_s symmetry geometries. For thymine, the geometrical parameters of the T_a conformation (Fig. 1, Table 1) have been used (see also Section 2.2.1). The calculated vibrational modes can be classified through A′ and A″ irreducible representations of the C_s point group: 30 vibrational modes (21 A′ in-plane and 9 A″ out-of-plane) from uracil and 39 vibrational modes from thymine (26 A′ and 13 A″) are expected.

The first set of vibrational wavenumbers calculated before using any scaling procedure is reported in Appendix A (Table 4) for both U and T. The scaled calculated wavenumbers and corresponding assignments based on the Potential Energy Distribution (PED) matrix, are presented in Tables 2 and 3 for U and T, respectively, and compared to the experimental wavenumbers.

2.2.4. NIS intensity simulations

In the simulation of the NIS intensities, we have used the same theoretical formalism and mathematical expressions as in our previous papers based on the NIS spectral analysis of adenine and guanine purine bases [1,2]. Here, we only mention the main approximations used, and the corresponding simulated spectra are reported in Figs. 3 and 4.

NIS peak intensities for the first-order interactions have been calculated in taking into account all atom (i.e. H, C, N and O) coherent and incoherent contributions. Obviously, hydrogen atom incoherent contributions are dominant, owing to its large incoherent cross-section. In Figs. 3 and 4 are shown the calculated first-order intensities of U and T (as shown by vertical lines, normalized to the strongest calculated peak). Moreover, the spectral shape of the first-order spectrum has been simulated by gaussian curves as shown in the lower part of Figs. 3 and 4. In order to account for the experimental resolution which rapidly decreases in the high-wavenumber region of the NIS spectra (above 1000 cm^{-1}), the half-width of the NIS gaussian bands has been supposed to be a quadratic function of the spectral wavenumber. Each of these simulated spectra (shown in the lower part of Figs. 3 and 4) has been normalized to its strongest band and compared with the experimental spectra in the region above the lattice modes.

3. Discussion

In the spectral region above 2500 cm^{-1}, which generally contains vibrational bands corresponding to N–H and C–H bond stretching motions, broad and poorly resolved bands are observed in the NIS spectra (not shown here). In contrast, in the optical spectra (IR and Raman) the intensities and resolution of the bands are good enough to analyse them accu-

Table 1
SCF + MP_2 molecular total energy (E_{tot}) along with zero point vibrational (Z.P.V.) energy (in atomic units: a.u.), obtained by using split-valence gaussian sets with different d-orbital polarization functions for carbon, nitrogen and oxygen. The calculated energies for different conformations of thymine (T_a, T_b, T_c and T_d) are indicated (see also Fig. 1 and text)

Molecule	Conformation	Point group	E_{tot} (a.u.)	Z.P.V. (a.u.)
uracil	U	C_s	−413.640008	0.0879
thymine	T_a	C_s	−452.815222	0.1166
	T_b	C_s	−452.813072	‡
	T_c and T_d	C_1	−452.814217	0.1164

‡: Conformation giving one imaginary vibrational wavenumber.

rately in the same spectral region. On the other hand, the C=O and C=C bond-stretching motions (usually featured between 1750 and 1600 cm^{-1}) are weak and probably superimposed with second- and higher-order NIS contributions (so-called multi-phonon NIS processes). For the sake of clarity,

Table 2
Comparison between experimental and calculated wavenumbers (obtained with SQM force fields) of uracil. For each calculated vibrational mode the corresponding assignment and potential energy distribution (PED in percent) in terms of internal coordinates, have been reported (PED values < 7% are not reported). C_s point group symmetry species (A′ or A″) to which each calculated vibrational modes belongs, are also indicated. ω and τ stand for wagging and torsional internal coordinates, respectively. See also Fig. 3 for the NIS intensities of most of the calculated vibrational modes

Experimental	Calculated	Assignments (PED in %)	Symmetry species
3485 [b]	3486	N1–H (100)	A′
3435 [b]	3436	N3–H (100)	A′
3130 [c], 3160 [d]	3145	C5–H (98)	A′
3080 [d], 3085 [c]	3082	C6–H (98)	A′
1716 [d]	1728	C2=O2 (43); C2–N1–H (9); C2–N3 (8); N1–C2 (7)	A′
1675 [d]	1691	C4=O4 (44); C5=C6(13); C4–C5 (11)	A′
1611 [c]	1626	C5=C6 (28); C4=O4 (21); N1C6H (14); C6–N1 (14); C5=C6H (11)	A′
1527 [a], 1508 [c,d]	1527	C2=O2 (27); C6N1H (16); C6–N1 (16); C2N1H (11)	A′
1450 [a], 1462 [c], 1453 [d]	1458	N3–C4 (18); C4–C5 (15); C2N1H (12); C6N1H (8)	A′
1417 [a], 1417 [d], 1422 [c]	1413	C5=C6 (14); C6=C5H (13); C4C5H (12); C5=C6H (11); N1–C2 (11); N1C6H (10)	A′
1370 [a] (sh), 1390 [d], 1398 [c]	1378	C4N3H (28); C2N3H (24); C2=O2 (20); C4=O4 (19)	A′
1251 [a]	1263	C6–N1 (20); C6=C5H (16); C4C5H (12); N3–C4 (9)	A′
1237 [a] (sh), 1236 [c], 1238 [d]	1233	C2–N3 (27); N3–C4 (19); N1–C2 (10); N1C6H (8)	A′
1104 [a], 1104 [c], 1099 [d]	1111	C6–N1 (26); C6=C5H (19); C5=C6 (15); C4C5H (12)	A′
1010 [c]	1011	N1C6C5 (16); C4=C5C6 (12); N3–C4 (8)	A′
1004 [a], 1003 [d]	1004	ω(C6H) (56); τ(C5=C6) (24); ω(C5H) (16)	A″
973 [a] (sh), 993 [d], 988 [c]	980	N1–C2 (23); C4–C5 (16); C2–N3 (12)	A′
870 [a] (sh), 875 [b]	873	ω(C5H) (49); ω(C4=O4) (28); ω(C6H) (13)	A″
831 [a], 842 [b]	833	ω(N3H) (54); τ(N3C2) (18); τ(N3C4) (14)	A″
771 [a]	767	ω(C4=O4) (43); ω(C6H) (21); ω(C2=O2) (19)	A″
781 [d], 792 [c]	763	C4–C5 (28); N1–C2 (20); C2–N3 (8)	A′
741 [a], 740 [b]	739	ω(C2=O2) (66); ω(C4=O4) (14)	A″
577 [a], 585 [d]	585	ω(N1H) (50); τ(N1C6) (27); τ(N1C2) (15)	A″
566 [a], 579 [c]	569	N1C2=O2 (22); N3C4=O4 (12); C5C4=O4 (9); N1C2N3 (8)	A′
565 [d], 558 [c]	552	N3C2=O2 (19); C5C4=O4 (13); C2N3C4 (9); N3–C4 (9); N1C2N3 (8)	A′
538 [a], 540 [c]	524	N3C4C5 (20); C6N1C2 (12); N3C4=O4 (12); C4C5=C6 (10)	A′
434 [a]	422	ω(C5H) (30); ω(C4=O4) (16); τ(C5=C6) (16); ω(N1H) (15); τ(N1C6) (10)	A″
398 [a](sh), 398 [c]	393	C5C4=O4 (18); N1C2=O2 (16); N3C2=O2 (14); N3C4=O4 (12); C2N3C4 (8); N3–C4 (8)	A′
201 [a]	170	ω(N1H) (35); τ(N3C2) (23); τ(N1C2) (15); ω(N3H) (9)	A″
166 [a]	155	ω(N3H) (47); τ(N3C4) (22); τ(C4C5) (16)	A″

[a] NIS spectrum, present work (Fig. 2).
[b] IR spectrum from Ar matrix (Ref. [13]).
[c] Raman spectra from polycrystalline samples (Ref. [6]).
[d] IR spectra from polycrystalline samples (Ref. [6]).

above 1600 cm^{-1} the calculated wavenumbers are only compared with those observed experimentally in IR and Raman spectra obtained from solid state phase or rare gas matrix. However, in the 1750–1600 cm^{-1} region the positions of the broad and non-structured NIS bands confirm the validity of our calculated wavenumbers and subsequent assignments.

Beyond the agreement between calculated and experimental wavenumbers (as it can be seen in Tables 2 and 3 and Figs. 3 and 4), one of the most striking point of this discussion concerns the comprehension of the differences arising between uracil and thymine NIS spectra as a consequence of H → CH_3 replacement at the 5-position of the pyrimidine ring (Fig. 1). This can be verified either by band shifts or new intense NIS bands as they appear in comparing the T and U spectra to each other. On the basis of normal mode assignments (Tables 2 and 3) and considering the experimental and calculated NIS intensities of U and T (Figs. 3 and 4), the origin of these spectral changes can be discussed as follows:

– In the 1550–1350 cm^{-1} spectral region, the T NIS spectrum yields additional bands (Fig. 2) as compared to the U one. Our calculations show (Table 3) that the methyl group angular deformations play an important role in this region: CH_3 anti-symmetric and symmetric angular bendings give rise to two intense NIS bands located at 1458 and 1387 cm^{-1}, respectively.

– The 1300 to 1100 cm^{-1} spectral region is also influenced by the presence of a methyl group at C5 position. There, the couplings of the C5–C(H_3) bond-stretching with the ring stretching and angular deformation motions are the most important. The U intense NIS doublet at 1251 cm^{-1} (simulated by two modes calculated at 1263 and 1233 cm^{-1}) is split in the case of T into two components peaking at 1262 and 1177 cm^{-1} (and calculated at 1271 and 1178 cm^{-1}, respectively). It should also be mentioned that the U intense band at 1104 cm^{-1} (calculated at 1111 cm^{-1}), involving C5–H angular bending contributions, does not exist in the T spectrum (Fig. 2).

– CH3-rocking motions alone or coupled with ring stretching motions of T give rise to two intense NIS bands at 1054 and 988 cm^{-1}, while the U spectrum yields a unique and prominent band at 1004 cm^{-1}, which mainly arises from C6–H out-of-plane wagging coupled with C5=C6 torsional and C5–H wagging vibrations. In T, the coupling of the C6–H wagging motions with adjacent C5=C6 torsional and C4=O4 wagging motions is responsible for the rather intense band at 945 cm^{-1}.

– Other important effects can be discussed by comparing the U and T spectra in the 900–700 cm^{-1} and 700–450 cm^{-1} spectral regions. In the former, the prominent 831 cm^{-1} band of U, broadened to higher wavenumbers (and mainly assigned to N–H and C=O waggings) is split into two components at 851 and 813 cm^{-1} in T. This is also a direct consequence of the presence of the methyl group in thymine. In the latter spectral region, the change in the couplings of N1–H wagging with the ring motions leads to a considerable upshift of the 577 cm^{-1} band of U, towards 646 cm^{-1} in T. One can explain other changes in this spectral region by the coupling of C5–C(H3) stretching and bending motions with the ring vibrations.

– In spite of quite different assignments (Tables 2 and 3), the resemblance of NIS intense bands observed at 434 cm^{-1} (U) and 431 cm^{-1} (T) (Figs. 2–4) should be underlined.

– NIS spectrum of uracil exhibits a broad gap between 250 and 400 cm^{-1}, while T spectrum yields two narrow bands at 286 and 323 cm^{-1}. Table 3 clearly shows that these modes originate from the in-plane and out-of-plane wagging modes in which the methyl group is considerably involved.

– Finally, internal modes located below 250 cm^{-1} have been assigned to out-of-plane motions in which the ring torsions and extracyclic waggings are strongly coupled. In particular, the most prominent NIS band seen at 174 cm^{-1} in T (calculated at 177 cm^{-1}) is assigned to the methyl group torsional mode (torsion around the C5–C(H3) chemical bond, Fig. 1).

4. Concluding remarks

An adequate SQM force field enabled vibrational data of uracil and thymine, obtained from different spectroscopical techniques (NIS, IR absorption and Raman scattering) to be interpreted. A good agreement between calculated and experimental wavenumbers has been achieved in the various spec-

tral regions. Considering the C_s geometry theoretically estimated for both molecules, we have assigned their vibrational modes through the A′ and A″ symmetry species of this point group. Moreover, by simulating the NIS band intensities, the validity of the atomic displacements predicted by the used molecular wavefunctions has been checked.

For A′ representation, the calculated results do not raise any particular difficulty. For instance, as far as the C–H and N–H bond-stretch motions are concerned, a quasi constant ratio of 0.96 (wavenumber scaling factors) has been found between experimental (Tables 2 and 3) and unscaled wavenumbers (Table 4). This is also true for other vibrational

Table 3
Same as Table 2 but for thymine. See also Fig. 4 for the NIS intensities of most of the calculated vibrational modes

Experimental	Calculated	Assignments (PED in %)	Symmetry species
3480 [b]	3481	N1–H (100)	A′
3434 [b]	3434	N3–H (100)	A′
3066 [c], 3063 [d]	3065	C6–H (99)	A′
2991 [c], 2993 [d]	2991	CH3–antisym. st.1 (99)	A′
	2991	CH3–antisym. st.2 (99)	A″
2934 [c], 2930 [d]	2932	CH3–sym. st.(100)	A′
1706 [c], 1735 [d]	1739	C2=O2 (38); C2N1H (11); N1–C2 (11); C2–N3 (8)	A′
1674 [c], 1677 [d]	1683	C5=C6 (29); C4=O4 (21)	A′
1600 [d]	1609	C4=O4 (38); C5=C6 (23); C4–C5 (9); C6–N1 (8)	A′
1510 [a], 1492 [c], 1495 [d]	1511	C2=O2 (23); C6N1H (15); C4=O4 (10); C2N1H (9)	A′
1485 [a], 1483 [d]	1484	N1–C2 (15); C2N1H (14); C2–N3 (10); C4–C5 (9); C6N1H (8)	A′
1458 [a], 1461 [c]	1465	CH3–antisym, bend. (80); CH3–antisym. rock. (10)	A′
1447 [a] (sh), 1447 [d]	1439	CH3–antisym. bend. (89)	A″
1406 [d], 1409 [c]	1389	CH3–antisym. bend. (16); C5=C6 (16); C5=C6H (15); N1C6H (12); C4–C5 (8)	A′
1387 [a], 1379 [c], 1383 [d]	1383	CH3–sym. bend. (71); C5–C(H3) (19)	A′
1366 [a] (sh), 1366 [d], 1370 [c]	1362	C2=O2 (26); C2N3H (23); C4=O4 (22); C4N3H (21)	A′
1262 [a], 1248 [c], 1245 [d]	1271	C5–C(H3) (20); C6–N1 (13); C2N3 (12); C4–C5 (10); N1–C2 (10); N1C6H (9)	A′
1224 [a], 1203 [d], 1216 [c]	1221	C6–N1 (31); C2–N3 (13); N1C6H (11); C6N1H (9)	A′
1177 [a], 1157 [c], 1152 [d]	1178	N3–C4 (36);C5–C(H3) (12)	A′
1054 [a]	1056	CH3–antisym.rock. (80)	A″
1028 [d]	1046	CH3–antisym.rock. (38); N1–C2 (10); C2–N3 (9)	A′
988 [a], 985 [c,d]	987	CH3–antisym. rock. (46); N1–C2 (10)	A′
945 [a]	945	ω(C6H) (60); τ(C5=C6) (14); ω(C4=O4) (10); τ(N1C6) (8)	A″
851 [a]	855	ω(N3H) (54); τ(N3C2) (13); τ(N3C4) (12)	A″
	824	C5–C5–C(H3) (27); C2=O2 (12); N1–C2 (9)	A′
813 [a], 815 [d]	814	ω(C4=O4) (43); ω(C2=O2) (32); ω(C5–CH3) (8)	A″
760 [a] (sh), 764 [b]	763	ω(C2=O2) (54); ω(C4=O4) (18); ω(C6H) (12)	A″
751 [a], 754 [b]	745	C4–C5 (34); C5–C(H3) (16)	A′
646 [a]	653	ω(N1H) (34); τ(N1C6) (32); τ(N1C2) (24)	A″
621 [a], 617 [c,d]	616	C5C4=O4 (19); N1C2=O2 (13); N3C2=O2 (11); C4C5C(H3) (8); C5=C6 (8)	A′
562 [a], 562 [c,d]	556	N3C4=O4 (13); C2N3C4 (12); N3C4C5 (9); N1C6C5 (9); N1C2=O2 (9); C2–N3 (9)	A′
479 [a], 475 [c,d]	479	C4C5=C6 (15); N3C2=O2 (12); N1C2N3 (11); C5–C(H3) (11); N3–C4 (9); N3C4C5 (8)	A′
431 [a]	426	ω(C5–CH3) (29); ω(N1H) (23); τ(C5=C6) (13); ω(C6H) (12); ω(C4=O4) (11)	A″

Table 3 (continued)

Experimental	Calculated	Assignments (PED in %)	Symmetry species
391 [b]	388	N1C2=O2 (19); C5C4=O4 (14); N3C2=O2 (13); N3C4=O4 (13)	A′
323 [a], 321 [c,d]	326	ω(C5–CH3) (49); ω(N1H) (15); CH3–antisym. rock. (9); τ(C5=C6) (8)	A″
286 [a]	290	C4C5C(H3) (38); C6=C5–C(H3) (29); C5C4=O4 (9); CH3–antisym. rock. (8)	A′
206 [a]	170	ω(N3H) (45); τ(C4C5) (18); τ (N3C4) (17); τ(N3C2) (9)	A″
174 [a]	177	τ(C5–CH3) (89)	A″
148 [a]	126	ω(N1H) (33); τ(C4C5) (19); τ(N3C2) (15); τ(N1C2) (12)	A″

[a–d] For footnotes see Table 2.

modes in which the bond-stretching contributions are predominant, with the exception of a slight overestimation of the calculated wavenumbers of the C=O bond-stretching modes giving a scaling factor of 0.92. The wavenumber scaling factors are even closer to unity for the in-plane modes mainly involving angular bendings.

In the case of the A″ representation, most of the calculated wavenumbers are underestimated (except for the methyl group vibrational values which have been overestimated). The scaling procedure led to increase the wagging and torsional force constants, so as to increase the corresponding calculated wavenumbers. However, it is worth to be mentioned that in NIS simulations a disagreement has been encountered for some of the A″ modes, specially those located below 600 cm^{-1}. In the case of uracil, the intensity of the mode observed at 577 cm^{-1} is largely overestimated in our simulation. The same kind of result has been observed for the 621 cm^{-1} thymine mode (Figs. 3 and 4). In contrast, NIS intensities as well as wavenumbers of the vibrational modes located below 200 cm^{-1} are too weak. It should be mentioned that all of these effects have also been observed in the unscaled initial force field, i.e. this giving rise to the vibrational wavenumbers reported in Table 4.

Several arguments can be found in order to explain these discrepancies:

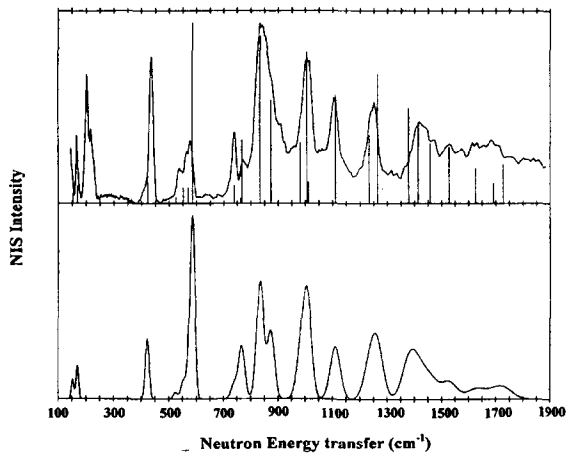

Fig. 3. Comparison between experimental (up) and simulated (down) NIS spectra of uracil in the region corresponding to internal molecular motions. Each of the spectra has been normalized to its most intense band. In the upper part, the first-order calculated NIS intensities are drawn as vertical lines.

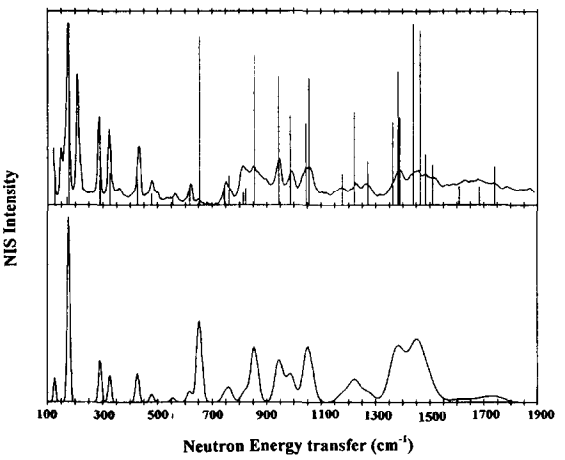

Fig. 4. Same as Fig. 3, but for thymine.

(i) NIS experiments are carried out in polycrystalline phase, where strong intermolecular hydrogen bonding and stacking effects may considerably perturb the molecular internal vibrational modes [9], while the calculated results presented here arise from a supposed isolated molecule, i.e. without interaction with any other,

(ii) low-wavenumber vibrations and specially those arising from A″ symmetry species, are often produced by large amplitude motions which cannot be easily interpreted by a harmonic normal coordinate treatment, and:

(iii) molecular orbital calculations, even using extended basis sets with polarization functions as do the present ones, may well be inefficient to explain correctly the A″ symmetry vibrational modes, specially those involving extracyclic wagging coordinates.

In order to clarify and validate these hypotheses, additional experimental (IR and Raman experiments in both solid and liquid phases, NIS spectra from deuterated molecular species) and theoretical investigations (ab initio calculations with appropriate polarization functions) are now in progress.

Table 4
Initial unscaled wavenumbers (cm^{-1}) for uracil and thymine molecules. For each wavenumber the symmetry species, to which the corresponding vibrational mode belongs, is reported(see also text)

Uracil		Thymine	
A′	A″	A′	A″
3656	930	3654	3190
3612	799	3610	1529
3304	738	3250	1089
3263	722	3201	880
1868	698	3104	747
1826	566	1867	730
1712	379	1805	697
1536	161	1736	568
1449	139	1554	377
1436		1533	292
1413		1471	149
1273		1458	143
1236		1420	109
1113		1413	
999		1284	
990		1238	
782		1190	
560		1045	
541		988	
518		814	
383		750	
		607	
		546	
		461	
		386	
		279	

5. Additional materials available

Calculated geometrical parameters (internal coordinates as well as atomic cartesian coordinates) of uracil and thymine, unscaled and scaled force constant matrices and scaling factor sets can be provided upon request.

Acknowledgements

All of the quantum chemical computations reported in this paper have been carried out on Cray C90 computers. The authors would like to thank IDRIS (Institut du Développement et des Ressources en Informatique Scientifique, CNRS) and Cray-Research France for access to computational facilities. A.A. is partly supported by a fellowship from the Government of Morocco. The authors thank the Rutherford Appleton Laboratory Staff for their technical assistance in using the TFXA to obtain NIS spectra.

Appendix A

In Table 4 we report the unscaled vibrational wavenumbers (as direct outputs from the GAUSSIAN code) of uracil and thymine, along with the corresponding symmetry species.

References

[1] Z. Dhaouadi, M. Ghomi, J.C. Austin, R.B. Girling, R.E. Hester, P. Mojzes, L. Chinsky, P.Y. Turpin, C. Coulombeau, H. Jobic and J. Tomkinson, J. Phys. Chem. 97 (1993) 1074.

[2] Z. Dhaouadi, M. Ghomi, Ce. Coulombeau, C. Coulombeau, H. Jobic, P. Mojzes, L. Chinsky and P.Y. Turpin, Eur. Biophys. J. 22 (1993) 225.

[3] B. Cadioli, E. Gallinella, C. Coulombeau, H. Jobic and G. Berthier, J. Phys. Chem. 97 (1993) 7844.
[4] E. Gallinella, B. Cadioli, J.P. Flament and G. Berthier, J. Mol. Struct. THEOCHEM 315 (1994) 137.
[5] C. Coulombeau and H. Jobic, J. Mol. Struct. THEOCHEM 330 (1995) 127.
[6] H. Susi and J.S. Ard, Spectrochim. Acta 27A (1971) 1549.
[7] H. Susi and J.S. Ard, Spectrochim. Acta 30A (1974) 1843.
[8] R.C. Lord and G.J. Thomas Jr., Spectrochim. Acta 23A (1967) 2551.
[9] J. Bandekar and G. Zundel, Spectrochim. Acta 39A (1983) 343.
[10] J. Florian and V. Hrouda, Spectrochim. Acta 49A (1993) 921.
[11] C.L. Angell, J. Chem. Soc. (1961) 504.
[12] A.J. Barnes, M.A. Stuckey and L. Le Gall, Spectrochim. Acta 40A (1984) 419.
[13] A. Les, L. Adamowicz, M.J. Nowak and L. Lapinski, Spectrochim. Acta 48A (1992) 1385.
[14] M. Szczesniak, M.J. Nowak, H. Rostkowska, K. Szczepaniak, W.B. Person and D. Shugar, J. Am. Chem. Soc. 105 (1983) 5969.
[15] S. Chin, I. Scott, K. Szczepaniak and W.B. Person, J. Am. Chem. Soc. 106 (1984) 3415.
[16] W.B. Person and K. Szczepaniak, in: Vibrational spectra and structure, Vol. 20, ed. J.R. Durig (Elsevier, Amsterdam, 1993) p. 239.
[17] B. Pullman and A. Pullman, in: Quantum biochemistry (Interscience, New York, 1963) p. 825.
[18] H. Berthod, C. Giesner-Prettre and A. Pullman, Theoret. Chim. Acta 5 (1966) 53.
[19] H. Berthod, C. Giesner-Prettre and A. Pullman, Intern. J. Quant. Chem. 1 (1967) 123.
[20] V.A. Kuprievich, Intern. J. Quant. Chem. 1 (1967) 561.
[21] C. Nagata, A. Imamura and H. Fujita, in: Advances in biophysics, ed. M. Kotani (Univ. Tokyo Press, Tokyo, 1977).
[22] W.D. Bowman and T.G. Spiro, J. Chem. Phys. 73 (1980) 5482.
[23] E. Clementi, J.M. André, M.C. André, D. Klint and D. Hahn, Acta Phys. Acad. Sci. Hung. 27 (1969) 493.
[24] Y. Nishimura, M. Tsuboi, S. Kato and K. Morokuma, J. Am. Chem. Soc. 103 (1981) 1354.
[25] M. Tsuboi, Y. Nishimura, A.Y. Hirakawa and W.L. Peticolas, in: Biological applications of Raman spectroscopy, Vol. 2, ed. T.G. Spiro (Wiley, New York, 1987) p. 109.
[26] J. Penfold and J. Tomkinson, Rutherford Appleton Laboratory Report, RAL-86-019, Rutherford Appleton Laboratory, Chilton (1988).
[27] J. Tomkinson, C.J. Carlile, S.W. Lovsey, R. Osbora and A.D. Taylor, in: Spectroscopy of advanced materials, eds. R.J.H. Clark and R.E. Hester (Wiley, Chichester, 1991) ch. 3.
[28] H. Jobic and H.J. Lauter, J. Chem. Phys. 88 (1988) 5450.
[29] E.B. Wilson Jr., J.C. Decius and P.C. Cross, in: Molecular vibrations (McGraw-Hill, New York, 1955).
[30] M. Gusoni and G. Zerbi, J. Mol. Spectry. 26 (1968) 485.
[31] F. Török, A. Hegedüs, K. Kosa and P. Pulay, J. Mol. Struct. 32 (1976) 93.
[32] G. Fogarasi and P. Pulay, in: Vibrational spectra and structure, Vol. 14, ed. J.R. Durig (Elsevier, Amsterdam, 1985) p. 125.
[33] W.J. Hehre, L. Radom, P. von R. Schleyer and J.A. Pople, in: Ab initio molecular orbital theory (Wiley, New York, 1986).
[34] M. Frisch, GAUSSIAN 90 User's Guide (Gaussian, Inc., Carnegie-Mellon University, 1990).
[35] R.F. Stewart and L.H. Jensen, Acta Cryst. 23 (1967) 1102.
[36] R. Gerdil, Acta Cryst. 14 (1961) 333.